Applying the Hoffmann-Hill criterion to short-fiber plastics

Johannes Selb. BSc., Dr. techn. Franz-Josef Falkner (supervisor)

***Abstract*—In cases where plastics are not strong enough to withstand loads, short-fibers are injected. However, the determination of failure in such parts is way more complex than in metals or other isotropic materials. Short-fiber composites have a fully orthotropic behavior and cannot be calculated with commonly used equivalent stress theories, such as the Von Mises yield criterion. Therefore, experimental determination of failure is the only accurate solution to date. This, however, is costly and time-consuming.**

In order to reduce cost and allow for a faster calculation of material failure for different load cases, a simulation workflow within ANSYS is established. ANSYS hereby yields a big library for short-fiber reinforced materials and also provides fundamental tools for defining the material at hand. Additionally, experimental data from tensile tests as well as an injection molding simulation is needed. This is used to define a new material model in ANSYS, which is fitted according to the experimental data.

To determine the equivalent stresses needed for static and fatigue analysis, a new failure model is added to ANSYS. Using ANSYS' integrated Python programming tool, internal variables are accessed and manipulated. These variables consist of stresses, element orientation, and eigenvalues that are needed in order to implement failure models suited for short-fiber plastics. Both Hofmann and Tsai-Hill failure criteria account for orthotropic materials with different strengths in tension and compression.

For a defined part with a complete injection molding simulation, a failure analysis within ANSYS is performed. For a defined workflow, the utilization rate will be compared to experimental data in order to proof the concept.

***Index Terms*—short-fiber plastics, failure, ANSYS, Python**

I. Introduction

WITH the technical evolution towards cheaper and more lightweight construction short fiber reinforced materials have become common in structural mechanics. This is underlined in the Short Fiber Thermoplastics Insight [1], which states that short-fiber reinforced plastics are continuing to grow in usage in the upcoming years. However, the determination of material failure has proven to be difficult. The orthotropic material behavior, which is present in short-fiber plastics, shows the limitations of the widely used Von Mises' yield criterion [2]. Over the years, many adaptations and different theories have been created in order to calculate failure in orthotropic material behavior. The Hill [3] criterion, a variation of the Von Mises' theorem, has been developed in order to account for different material strengths in different directions. This already provides a higher accuracy than the Von Mises' criterion. However, a closer inspection during material testing shows a deviation of compression and tension within the material. This material behavior also known as the Bauschinger effect, has been implemented by Hoffmann [4]. The Hoffmann criterion hereby yields a compact way for calculating material failure in short-fiber reinforced plastics. The Hoffmann yield criterion is not the only available solution in order to solve a finite element model of a short-fiber reinforced plastic. Tsai [5] has also developed an adaptation for calculating short-fiber plastics based on the Hill criterion. This approach is different from the one of Hoffmann and considers the difference in compression and tension by applying different strengths under different load cases. Tsai and Wu [6] further implemented the Tsai-Wu criterion, which can be used for any material behavior and is not limited to orthotropic material behavior. The Tsai-Wu criterion is a tensor-based failure model where all 27 material constants would be needed in order to calculate failure for a fully anisotropic material. The application of these different failure models stays complex since they require a lot of information about the material at hand. The information about the fiber direction within the material, which is determined during the injection molding process, is still a complex task. Modern software such as Moldex3D [7] can provide information about the injection molding process. In order to combine the different frameworks, ANSYS [8] is used to calculate previously stated failure theories on complex geometries. ANSYS already

provides many tools for material definition and has already implemented important functions in order to solve short-fiber reinforced plastics [9].

II. Theoretical Background

A. Material Behavior

Every material can be assigned into a class of material behavior. The simplest of them being isotropic material behavior. Isotropic materials show the same material strength in every direction. This can be shown by the strength tensor

$$F_{ij} = F_{11} \begin{bmatrix} 1 & -\frac{1}{2} & -\frac{1}{2} & 0 & 0 & 0 \\ & 1 & -\frac{1}{2} & 0 & 0 & 0 \\ & & 1 & 0 & 0 & 0 \\ & & & 3 & 0 & 0 \\ & & & & 3 & 0 \\ & & & & & 3 \end{bmatrix} \tag{1}$$

with F_{11} being the strength of the material [6]. Orthothropic materials already show a larger degree of complexity

$$F_{ij} = \begin{bmatrix} F_{11} & F_{12} & F_{13} & 0 & 0 & 0 \\ & F_{22} & F_{23} & 0 & 0 & 0 \\ & & F_{33} & 0 & 0 & 0 \\ & & & F_{44} & 0 & 0 \\ & & & & F_{55} & 0 \\ & & & & & F_{66} \end{bmatrix} \tag{2a}$$

$$F_i = \begin{Bmatrix} F_1 \\ F_2 \\ F_3 \\ 0 \\ 0 \\ 0 \end{Bmatrix} \tag{2b}$$

with F_i being the material strength tensor of second rank, used to account for internal stresses. F_{ij} is used in order to describe the material strength of fourth rank due to outside loading. This material behavior shows different strengths in normal and shear directions, as well as coupling between the normal stresses [6]. In order to describe a fully anisotropic material

$$F_{ij} = \begin{bmatrix} F_{11} & F_{12} & F_{13} & F_{14} & F_{15} & F_{16} \\ & F_{22} & F_{23} & F_{24} & F_{25} & F_{26} \\ & & F_{33} & F_{34} & F_{35} & F_{36} \\ & & & F_{44} & F_{45} & F_{46} \\ & & & & F_{55} & F_{56} \\ & & & & & F_{66} \end{bmatrix} \tag{3a}$$

$$F_i = \begin{Bmatrix} F_1 \\ F_2 \\ F_3 \\ F_4 \\ F_5 \\ F_6 \end{Bmatrix} \tag{3b}$$

is used with different strengths in all directions for internal and external stresses, as well as coupling along every direction [6]. This level of complexity is rarely needed and therefore can mostly be simplified to orthotropic material behavior.

B. Difference of Compression and Tension

Some materials show different strengths in tension and compression. This is based on two basic mechanisms. The first one is mainly present in treated metals and forces usually isotropic materials into anisotropy. This effect is called the Bauschinger effect [10].

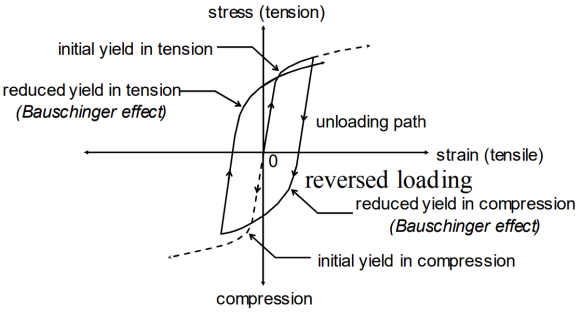

Fig. 1. Effect of the Bauschinger effect [11]

Figure 1 shows the result of the Bauschinger effect. Once the material is loaded above the elastic limit, plastic deformation of the material is occurring, which increases the yield strength in the loading direction. However, the strength opposite of the loading direction is reduced.

Another mechanism that results in a difference in tension and compression is explained by Carter and Norton [12]. This mechanism is mainly present in ceramics; however, it can be adapted for other materials as well. The material behavior is dominated by flaws, such as cracks, pores, and empty spaces.

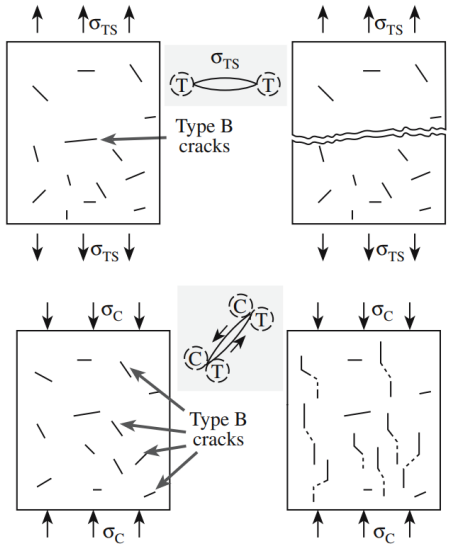

Fig. 2. Critical Cracks under different loading conditions [12]

Figure 2 shows critical cracks for ceramic materials under tensile and compressive loading. Different cracks will result in earlier material failure under tensile and compressive loading. Under compressive loading, critical cracks twist and stably propagate along the compressive axis, which will crush the material rather than fracture it. Under tensile loading, the critical flaw is oriented differently and has a higher impact on material failure. These flaws result in an unstable fracture of the material since the crack is quickly opened up, thus increasing the size of the crack instead of closing it. Because of these mechanisms, ceramics show a higher strength in compression [12]. The same mechanisms can be applied to short-fiber reinforced plastics.

C. Yield Criteria

Based on the yield criterion of Von Mises, Hill adapted it to account for different strengths in different directions. Hills yield stress criterion reads as

$$\hat{\sigma} = \sqrt{\begin{aligned} &F\left(\sigma_{22}-\sigma_{33}\right)^2 + G\left(\sigma_{33}-\sigma_{11}\right)^2 \\ &+H\left(\sigma_{11}-\sigma_{22}\right)^2 + 2L\sigma_{23}^2 + 2M\sigma_{31}^2 + 2N\sigma_{12}^2 \end{aligned}} \tag{4}$$

with σ_{ii} being the normal stresses and σ_{ij} being the shear stresses. Constants F, G, H, L, M, and N describe the directional material strength parameters. These are determined using parameters of the injection molding simulation [13]. The Tsai-Hill criterion further implements the difference in tension and compression

$$\begin{aligned} 1 = &\frac{\sigma_{11}^2}{X^2} + \frac{\sigma_{22}^2}{Y^2} + \frac{\sigma_{33}^2}{Z^2} \\ &- \left(\frac{1}{X^2} + \frac{1}{Y^2} - \frac{1}{Z^2}\right)\sigma_{11}\sigma_{22} \\ &- \left(\frac{1}{X^2} - \frac{1}{Y^2} + \frac{1}{Z^2}\right)\sigma_{11}\sigma_{33} \\ &- \left(-\frac{1}{X^2} + \frac{1}{Y^2} + \frac{1}{Z^2}\right)\sigma_{22}\sigma_{33} \\ &+ \frac{\sigma_{12}^2}{S_{12}^2} + + \frac{\sigma_{23}^2}{S_{23}^2} + + \frac{\sigma_{13}^2}{S_{13}^2} \end{aligned} \tag{5}$$

where the normal strengths X, X, and Z can be adapted to positive or negative normal stress, thus giving the opportunity to consider different behaviors in compression and tension [14]. Tsai and Wu further developed the Tsai-Wu criterion for orthotropic materials

$$\begin{aligned} 1 = &F_1\sigma_1 + F_2\sigma_2 + F_3\sigma_3 \\ &+ F_{11}\sigma_1^2 + F_{22}\sigma_2^2 + F_{33}\sigma_3^2 \\ &+ 2F_{12}\sigma_1\sigma_2 + 2F_{13}\sigma_1\sigma_3 + 2F_{23}\sigma_2\sigma_3 \\ &+ F_{44}\sigma_4^2 + F_{55}\sigma_5^2 + F_{66}\sigma_6^2 \end{aligned} \tag{6}$$

where the simplifications for orthotropic materials as mentioned in chapter II-A come into place [6]. The material parameters F_{ij} should be obtained experimentally; however, approximations exist. With these approximations, it is possible to calculate F_{ij} with normal strength in x, y, and z directions in tension and compression as well as shear strengths [15]. The yield criterion considered last is the Hoffmann criterion. Hoffmann adapted the yield criterion of Hill

$$\begin{aligned} 1 = &C_1\left(\sigma_y-\sigma_z\right)^2 + C_2\left(\sigma_z-\sigma_x\right)^2 + C_3\left(\sigma_x-\sigma_y\right)^2 \\ &+ C_4\sigma_x + C_5\sigma_y + C_6\sigma_z + C_7\tau_{yz}^2 + C_8\tau_{zx}^2 + C_9\tau_{xy}^2 \end{aligned} \tag{7}$$

where the linear terms in the equation are used to describe the Bauschinger effect, thus a difference in tension and compression [4].

D. Experimental Data

In order to gain material information, it is necessary to perform experiments. The most common experiment for material testing is a uniaxial tensile/compression test.

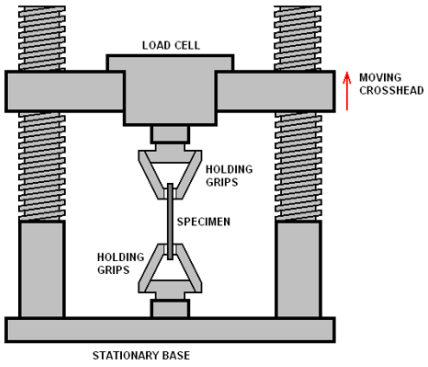

Fig. 3. Schematic of a tensile/compression test [16]

Figure 3 shows the schematic of a tensile/compression test. A specifically shaped specimen is held into place by holding grips, which are specially designed to hold the geometry of the specimen in place. A moving crosshead is then used to apply a load on the specimen, where the direction determines if it is a tensile or compression test. While the crosshead applies the load on the specimen, the traveled distance of the crosshead as well as the applied force are measured.

III. Objectives

The aim of this thesis is the establishment of a workflow within ANSYS in order to calculate material failure of complex short-fiber reinforced plastic parts.

Hereby, different failure models are implemented and tested against experimental data to identify the model that is best suited for the application.

IV. Methods

A. Injection Molding Simulation

Modern injection molding simulations provide many powerful tools in order to predict or post-process the molding process. Areas of low material flow or areas with problematic cooling can be identified and optimized using injection molding simulations. Important for this thesis is the fiber orientation in every position of the part as well as the mesh used in this simulation. These are important informations when it comes to characterizing the material within ANSYS.

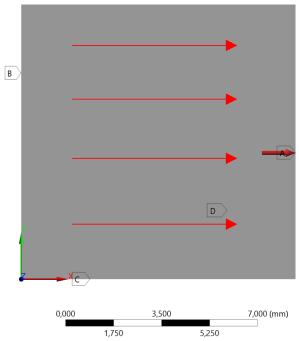

Fig. 4. Unit Cube with fibers along x-direction

Figure 4 displays a unit cube where the injection molding file has been edited and the fibers are fully oriented in the x-direction. For this thesis, the software Moldex3D [7] has been used in order to generate the mesh and orientation file.

B. ANSYS

ANSYS is used in order to combine external data, such as geometry, injection molding simulation and Python code. ANSYS provides a wide range of tools that are needed to implement the final workflow. Within Workbench, blocks are used to provide functionality that can be connected for a complete workflow. The most important blocks are the Material Designer block, the injection molding simulation block, and the static structural block. The Material Designer block gives the ability to adjust the material according to experimental datasets and gives the opportunity for an optimization to fit the material to the experimental data [13]. The injection molding simulation block allows the user to insert the fiber orientation file as well as the mesh file for the used geometry. These blocks are connected to the related parts of the static structural block, where all functions are combined. Inside the static structural block the finite element model has to be built up before the failure model can be used.
In ANSYS Mechanical, which will be opened upon clicking on the static structural block, the failure model is added using Python Results. Python Results are used to access ANSYS' internal variables, such as fiber orientation, stresses, fields, etc. Furthermore, an IronPython coding environment is provided where custom code can be added. By the use of operators, ANSYS' internal variables can be used and overwritten, which makes it possible to calculate the equivalent stresses mentioned in chapter II-C. Contour plots are plotted, which allows the user to evaluate material failure in every location of the part.

C. Visual Studio Code

Evaluation of failure can be performed in Visual Studio Code as well. For that, the workpath of the current result file of ANSYS has to be used to access the result file in Visual Studio Code. Furthermore, PyAnsys [17]needs to be added to provide important functionalities, such as accessing the stresses and fiber orientation. PyAnsys includes ANSYS native operators, which are also used in the Python Result. Visual Studio Code; however, does not offer the same analysis tools such as Slicing and Path Analysis.

D. Plastic Tensile Test

Although the working principle of tensile tests of plastics is the same, compared to metals, there are some differences to be considered. Metal test specimens have a cylindrical geometry, which cannot be found for plastic tensile tests. In fact, the geometry of the plastic tensile test is also dependant on the type of plastic that is used. This is in agreement with DIN EN ISO 527-1 [18], particularly EN ISO 527-4 [19], which describes the tensile test for short-fiber reinforced plastics.

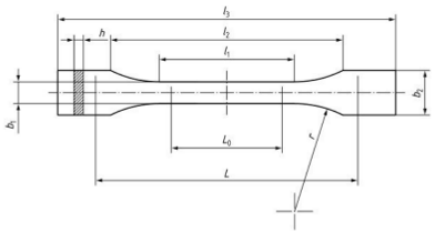

Fig. 5. Geometry of a plastic tensile test specimen DIN EN ISO 527-4 [19]

Figure 5 shows the geometry of a specimen suited for short fiber plastics. In order to deliver sufficient data to characterize a material, the specimen has to be cut out of a defined plate with known fiber direction.

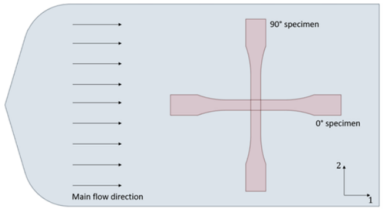

Fig. 6. Orientation of the manufactured specimen [13]

The main directions, as can be seen in Figure 6, have to be cut out at an angle of $0°$ and $90°$ towards the fiber direction. To prevent outliers from influencing the measurement, DIN EN ISO 527-1 [18] orders the same orientation to be tested at least five times.

V. Results

A. Single-Element Test

In order to check the proper implementation of the failure criteria and the workflow in general, a single-element test is performed. A single-element test is an analysis that only uses one element in a finite element analysis. This leads to a more understandable result.

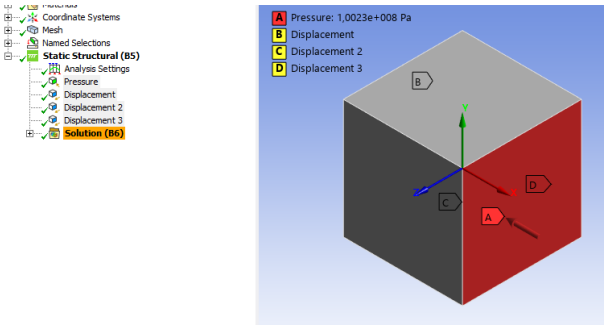

Fig. 7. Assigned constraints and loads

The single-element test, depicted in Figure 7, is fixed by three displacements, which reduces the degrees of freedom. Because of this, the cube is not able to perform a rigid body motion. Stresses are achieved by applying pressure to one of the corresponding axes, with the x-axis being the fiber-reinforced direction. The pressure corresponds to the tensile strength of the material.

B. Comparison of the Models

The single-element test is evaluated for different compressivity factors in $0°$ and $90°$ to fiber direction. The part is loaded with a pressure equivalent to the tensile strength; hence, failure is expected.

TABLE I
Comparison of failure criteria in tension and compression for a compressivity of 1

Failure Criterion	Tension	Compression
Tsai-Hill $0°$	0.2715	0.2715
Tsai-Wu $0°$	0.2715	0.2715
Hoffmann $0°$	0.2715	0.2715
Tsai-Hill $90°$	1	1
Tsai-Wu $90°$	1	1
Hoffmann $90°$	1	1

Table I shows the utilization rate of the test. It can be observed that failure $90°$ to fiber direction

can be reported. In the fiber direction, the material strength is higher because of the injected fibers. In this experiment, no compressivity is assumed, so no difference in tension or compression is observed.

TABLE II
COMPARISON OF FAILURE CRITERIA IN TENSION AND COMPRESSION FOR A COMPRESSIVITY OF 1.3

Failure Criterion	Tension	Compression
Tsai-Hill 0 °	0.2715	0.1606
Tsai-Wu 0 °	0.3291	0.0886
Hoffmann 0 °	0.3291	0.0886
Tsai-Hill 90 °	1	0.5917
Tsai-Wu 90 °	1	0.5385
Hoffmann 90 °	1	0.5385

By applying a small difference in tensile and compressive strength, the values already differ significantly, as can be seen in Table II. While the utilization on tension still shows failure in 90 ° towards fiber direction, there is also a difference in fiber direction. This comes from the calculation of the parameters that are used in the calculation of the stress. Compression shows a notable difference since the compressivity is squared, which results in a large deviation.

TABLE III
COMPARISON OF FAILURE CRITERIA IN TENSION AND COMPRESSION FOR A COMPRESSIVITY OF 1.5

Failure Criterion	Tension	Compression
Tsai-Hill 0 °	0.2715	0.1207
Tsai-Wu 0 °	0.3547	0.0073
Hoffmann 0 °	0.3547	0.0073
Tsai-Hill 90 °	1	0.4444
Tsai-Wu 90 °	1	0.3333
Hoffmann 90 °	1	0.3333

Further increasing the compressivity, as can be seen in Table III, only increases this trend.

TABLE IV
COMPARISON OF FAILURE CRITERIA IN TENSION AND COMPRESSION FOR A COMPRESSIVITY OF 2

Failure Criterion	Tension	Compression
Tsai-Hill 0 °	0.2715	0.0679
Tsai-Wu 0 °	0.3963	-0.1248
Hoffmann 0 °	0.3963	-0.1248
Tsai-Hill 90 °	1	0.25
Tsai-Wu 90 °	1	0
Hoffmann 90 °	1	0

However, when a compressivity of 2 is reached, Tsai-Wu and Hoffmann run into issues. This can clearly be seen in Table IV, where zero or negative entries emerge for the compressive load. This does not reflect real application and therefore reaches the limit of the computation method.

C. Testing of Real Part

The failure criteria are applied to a Stihl handlebar lock. The handlebar lock is tested for static failure of an applied load. The handlebar lock is used as a connection between two other parts; hence, failure of this part would cause significant damage to the product.

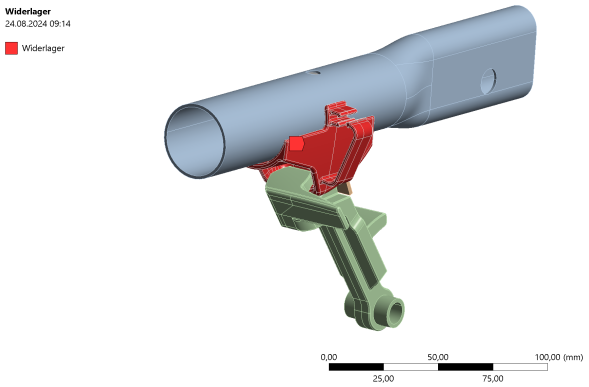

Fig. 8. Place of handlebar lock, tested for failure with the developed failure criteria

The simulation considers the assembly shown in Figure 8. It consists of three main parts; however, only the 'Widerlager' highlighted in red is considered for computation. The 'Widerlager' is the connection of the two other parts; hence, every force is transmitted by this part.

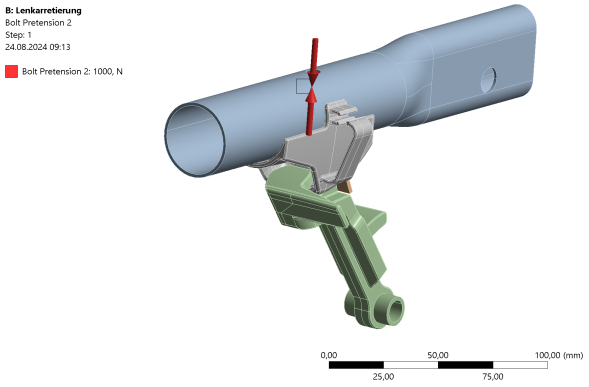

Fig. 9. Application of the bolt pretension to account for the assembled state

In order to fix the upper part to the structure, a bolt is inserted and tightened with 1000 N. This,

as displayed in Figure 9, results in a force on the 'Widerlager'.

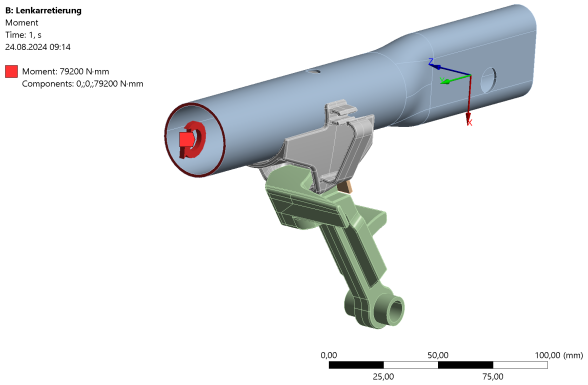

Fig. 10. Application of a torque in order to simulate a load case of the unit

Furthermore, a load is added by applying torque to the bar of the assembly. The torque shown in Figure 10 has an amplitude of $79\,200\,\mathrm{Nmm}$.

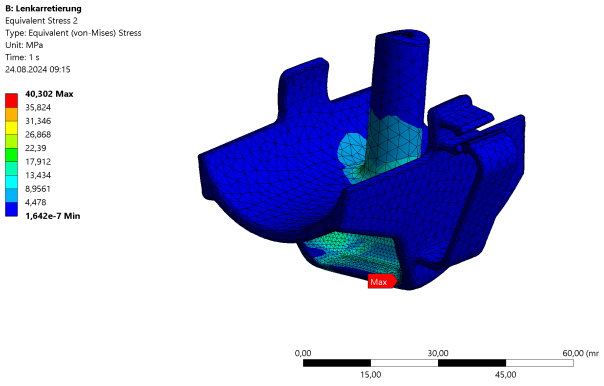

Fig. 11. Evaluation of material failure using the von Mises failure criterion

Evaluating the commonly used von Mises equivalent stress yields a maximum stress of $40.302\,\mathrm{MPa}$. When a tensile yield strength of $100.23\,\mathrm{MPa}$ is considered, this will result in a utilization of 0.402. However, this result does not account for orthotropic material behavior or a difference in tension and compression.

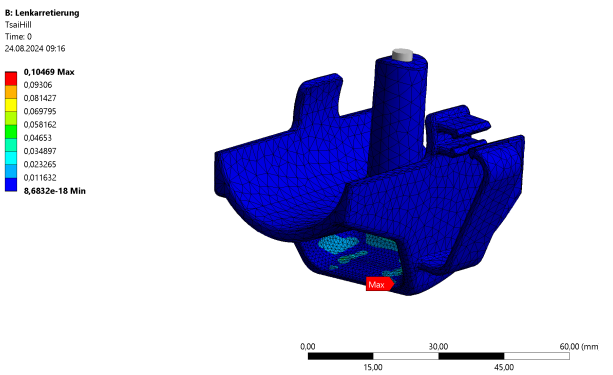

Fig. 12. Evaluation of material failure using the Tsai-Hill failure criterion

Figure 14 shows the utilization rate of the 'Widerlager' using the Tsai-Hill criterion. The computation was done using the same tensile yield strength and a compressivity of 1.2. Using the Tsai-Hill criterion, the maximum utilization is significantly smaller than with the von Mises criterion. This is because of the increased strength of the material due to injected fibers, as well as the increased compressive strength. Tsai-Hill yields a maximum stress of 0.105.

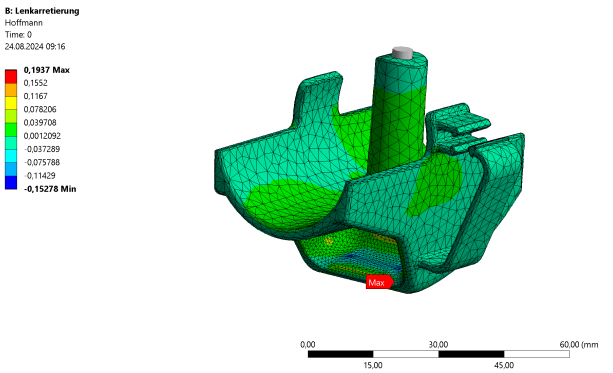

Fig. 13. Evaluation of material failure using the Hoffmann failure criterion

Switching the failure criterion to the Hoffmann criterion, as can be seen in Figure 13, changes the results considerably. Not only does the Hoffmann criterion produce negative values, but it also delivers much higher values than the Tsai-Hill criterion. The maximum stress of the Hoffmann yield criterion is 0.194, and the minimum is -0.153.

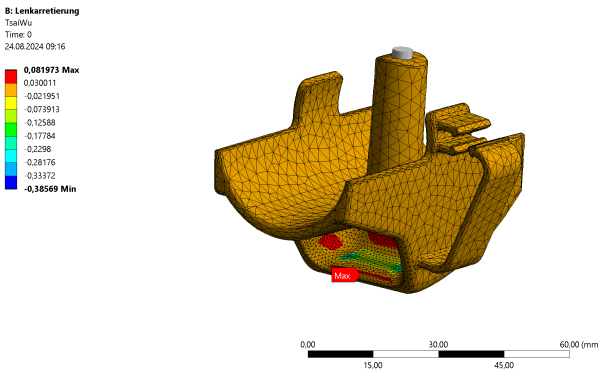

Fig. 14. Evaluation of material failure using the Tsai-Wu failure criterion

The Tsai-Wu criterion, depicted in Figure 14, shows the utilization of the 'Widerlager'. As with the Hoffmann criterion, both positive and negative values exist, with the negative maximum utilization being significantly larger. Tsai-Wu produces a maximum utilization of 0.082 and a minimum of -0.386.

VI. Conclusion

To conclude, it is possible to develop a workflow for evaluating failure in short-fiber reinforced plastics. When testing the failure criteria on a single-element test, largely expected values are calculated, which also match the theory. However, especially the Tsai-Wu and Hoffmann criterion show some flaws. For the single-element test, no utilization is predicted when a compressivity of 2 is applied. However, this would not be the case in reality. The same criteria also show unexpected results for the handlebar lock and can therefore not be used to evaluate failure unless more experimental testing is performed.

Future work in this field urges the need for more experimental testing and also evaluating more parts. The current state has little information about the real behavior, so only expectations are used for validation. Hence the accuracy and especially the applicability of the criteria cannot be verified. Furthermore, the workflow can be further optimized by applying new features of ANSYS, since the current state requires good knowledge of the proposed workflow.

References

[1] T. M. Research, "Short fiber thermoplastics market insights, 2021-2031," 2024, accessed: 2024-08-20. [Online]. Available: https://www.transparencymarketresearch.com/short-fiber-thermoplastics-market.html

[2] R. v. Mises, "Mechanik der festen körper im plastisch-deformablen zustand," *Nachrichten von der Gesellschaft der Wissenschaften zu Göttingen, Mathematisch-Physikalische Klasse*, vol. 1913, pp. 582–592, 1913.

[3] R. Hill, *The Mathematical Theory of Plasticity*, ser. Oxford Classic Texts in the Physical Sciences. Oxford, New York: Clarendon Press, 1998.

[4] O. Hoffman, "The brittle strength of orthotropic materials," *Journal of Composite Materials*, vol. 1, no. 2, pp. 200–206, 1967.

[5] S. W. Tsai and V. D. Azzi, "Anisotropic strength of composites," *Experimental Mechanics*, vol. 5, no. 9, pp. 283–288, 1965.

[6] S. W. Tsai and E. M. Wu, "A general theory of strength for anisotropic materials," Air Force Materials Laboratory, St. Louis, MO, Tech. Rep., 1972.

[7] Moldex3D, "Plastic Injection Molding Simulation," 2024, accessed: 2024-08-20. [Online]. Available: https://www.moldex3d.com/

[8] Ansys Inc., "Engineering Simulation Software," 2024. [Online]. Available: https://www.ansys.com/

[9] ——, "Short fiber composites tutorials," Southpointe, 2023.

[10] J. Bauschinger, "Über die veränderung der elastizitätsgrenze und der festigkeit des eisens und stahls durch strecken und quetschen, durch ermüdung und abkühlung und durch oftmaliges wiederholen dieser beanspruchungen," *Mittheilungen aus dem Mechanisch-Technischen Laboratorium der Königlichen Technischen Hochschule in München*, vol. 13, 1886.

[11] S. U. Pillai and D. Menon, *Reinforced Concrete Design*, 3rd ed. McGraw-Hill Education, 2018.

[12] C. B. Carter and M. G. Norton, *Ceramic Materials: Science and Engineering*, 2nd ed. New York, NY: Springer, 2013.

[13] Ansys Inc., "Material designer user's guide," Southpointe, 2022.

[14] I. Ansys, "Composites beta features," Southpointe, 2024.

[15] N. T. Mascia, E. A. Nicolas, and R. Todeschini, "Comparison between tsai-wu failure criterion and hankinson's formula for tension in wood," in *Proceedings of the 2011 International Conference on Composites*, Campinas, Brazil, 2011.

[16] ENGINEERING ARCHIVES, "Tensile Test," 2012. [Online]. Available: https://www.engineeringarchives.com/les_mom_tensiletest.html

[17] Ansys Inc., "PyAnsys," 2024, accessed: 2024-08-12. [Online]. Available: https://docs.pyansys.com/

[18] *Plastics - Determination of tensile properties - Part 1: General principles (ISO 527-1:2012)*, DIN Deutsches Institut für Normung e.V. Std. DIN EN ISO 527-1:2019-12, 2019.

[19] *Plastics - Determination of tensile properties - Part 4: Test conditions for isotropic and anisotropic fibre-reinforced plastic composites (ISO 527-4:2021)*, CEN European Committee for Standardization Std. EN ISO 527-4:2023-04, 2023.

Johannes Selb is a Master's student in the Department of Mechatronics at MCI Innsbruck, Austria. The topic of his work is largely in Software-based-evaluation of orthotropic material failure.